X-ray photon-counting using silicon photomultiplier-based scintillation detectors at high x-ray tube currents

Van Der Sar, Stefan; Brunner, Stefan; Schaart, Dennis

DOI
10.1117/12.2611365

Publication date
2022

Document Version
Final published version

Published in
Progress in Biomedical Optics and Imaging - Proceedings of SPIE

PROCEEDINGS OF SPIE

SPIEDigitalLibrary.org/conference-proceedings-of-spie

X-ray photon-counting using silicon photomultiplier-based scintillation detectors at high x-ray tube currents

van der Sar, Stefan, Brunner, Stefan, Schaart, Dennis

Stefan van der Sar, Stefan Brunner, Dennis Schaart, "X-ray photon-counting using silicon photomultiplier-based scintillation detectors at high x-ray tube currents," Proc. SPIE 12031, Medical Imaging 2022: Physics of Medical Imaging, 120310I (4 April 2022); doi: 10.1117/12.2611365

SPIE.

Event: SPIE Medical Imaging, 2022, San Diego, California, United States

X-ray Photon-Counting Using Silicon Photomultiplier-Based Scintillation Detectors at High X-ray Tube Currents

Stefan J. van der Sar[a*], Stefan E. Brunner[b], Dennis R. Schaart[a,c]
[a]Dept. of Radiation Science and Technology, Delft University of Technology, Mekelweg 15, 2629 JB, Delft, the Netherlands; [b]Broadcom Inc., Wernerwerkstrasse 2, 93049, Regensburg, Bavaria, Germany; [c]Holland Proton Therapy Center, Huismansingel 4, 2629 JH, Delft, the Netherlands.

ABSTRACT

We investigate fast scintillation detectors with silicon photomultiplier (SiPM) readout as a potential alternative to direct-conversion detectors based on CdTe, CdZnTe (CZT), and Si for X-ray photon-counting applications. Scintillation detectors may circumvent issues related to cost-effective growth of detector-grade material (CdTe, CZT) and detection efficiency (Si). Here, we experimentally study the count rate performance of two SiPM-based scintillation detectors and compare with direct-conversion detectors. We also study the energy response of the detectors.

We built 1×1 mm^2 single-pixel detectors consisting of the fast and commercially available $Lu_{1.8}Y_{0.2}SiO_5$:Ce (LYSO) and $YAlO_3$:Ce (YAP) scintillators and ultrafast SiPM prototypes. We irradiated both detectors using an X-ray tube and measured energy spectra, as well as observed count rates (OCR) as a function of tube current.

The measured spectra showed signs of the typical features of X-ray tube spectra. Using a 30 keV counting threshold, we measured maximum OCRs of 4.5 Mcps/pixel (LYSO) and 5.5 Mcps/pixel (YAP) for paralyzable-like counting, and OCRs approaching 10 Mcps/pixel (LYSO) and 12.5 Mcps/pixel (YAP) for nonparalyzable-like counting. These OCRs may be sufficient for some applications, but CdTe/CZT detectors highly optimized for photon-counting computed tomography (CT) achieve 10-15 Mcps/pixel (paralyzable-like) or 25-30 Mcps/pixel (nonparalyzable-like). Extrapolating our results, we estimate that such OCRs come within reach when using the twice as fast, and commercially available, $LaBr_3$:Ce scintillator.

In conclusion, we demonstrate X-ray photon-counting at count rates of multiple Mcps/pixel using SiPM-based scintillation detectors. Depending on the application-specific requirements, pixel size miniaturization may be necessary, for which we discuss two dose-efficient implementations.

Keywords: X-ray photon-counting, scintillator, silicon photomultiplier (SiPM), count rate performance, energy response

1. INTRODUCTION

The development, implementation and evaluation of photon-counting detectors (PCDs) for medical X-ray imaging systems, in particular for computed tomography (CT), has become a hot topic of research.[1,2] PCDs aim to count each detector pulse generated by a single X-ray photon and to assign it to one of a few energy bins, such that spectral/multi-energy X-ray imaging becomes possible. This is a challenging task, however, because the incident X-ray photon fluence rate can exceed 10^8 photons/mm^2/s,[3] such that pulse pile-up is likely to affect the measurement of counts and energies. In addition, an efficient X-ray absorber is needed as the maximum photon energy can be as high as 150 keV.

PCDs currently under consideration are based on the principle of direct conversion, i.e., each X-ray photon absorbed in a semiconductor, such as CdTe,[4] CdZnTe (CZT)[5] or Si[6], is directly converted into a number of electron-hole (e-h) pairs. This number is proportional to the energy deposited by the X-ray photon. Under the influence of an electric field, the charge carriers travel to (pixelated) electrodes on which they induce a current pulse. The front-end electronics outputs a (semi-)Gaussian shaped pulse, the height of which is a measure of the energy of the detected X-ray photon. This detector

* E-mail: s.j.vandersar@tudelft.nl; Phone: +31 15 278 3776.

Medical Imaging 2022: Physics of Medical Imaging, edited by Wei Zhao, Lifeng Yu, Proc. of SPIE
Vol. 12031, 120310I · © 2022 SPIE · 1605-7422 · doi: 10.1117/12.2611365

concept provides pulse durations in the order of tens of nanoseconds and facilitates pixel size miniaturization, both of which help to reduce pulse pile-up. However, the cost-effective growth of CdTe and CZT with a sufficiently low density of charge trapping centers (necessary to guarantee stable and reliable detector performance over time) remains an issue,[2,7] despite considerable progress over the past decades. Si detectors, on the other hand, face challenges related to the low mass density (ρ=2.3 g cm^{-3}) and atomic number (Z=14) of silicon. It is therefore not clear yet what the best choice of detector is, leaving room for the development of other detector concepts.

We are investigating such an alternative concept, namely very fast scintillation detectors with silicon photomultiplier (SiPM) readout. This type of detector relies on the principle of indirect conversion, i.e., a scintillator converts an absorbed X-ray photon into a pulse of optical scintillation photons, which is in turn converted into a current pulse by an SiPM (see figure 1a). The scintillation light pulse incident on the SiPM may be described as $A_1\exp(-t_1/\tau_d)$, with amplitude A_1 depending on the energy deposited by the X-ray photon, t_1 the time since the interaction of the X-ray photon, and τ_d the scintillation decay time constant. Much shorter τ_d than those of CsI (1 µs) and GOS (2.5 µs), which are used in energy-integrating X-ray detectors, are needed to minimize pile-up.[8]

Each scintillator pixel must be coupled to its own SiPM, which consists of a two-dimensional array of single-photon avalanche diodes (SPADs, see figure 1b). The absorption of a single optical photon from the scintillation pulse in a SPAD yields an e-h pair that can trigger a self-quenched avalanche multiplication process, yielding a gain in the order of 10^6. The current pulse from the SPAD may be described as $A_2\exp(-t_2/\tau_r)$, with A_2 the amplitude, t_2 the time since the detection of the optical photon and τ_r the recharge time constant. Since all SPADs on a single SiPM are connected in parallel, a detector output pulse may be described as a convolution of $A_1\exp(-t_1/\tau_d)$ and $A_2\exp(-t_2/\tau_r)$ (see figure 2a), the height of which is a measure of the energy of the detected X-ray photon. The internal gain of the SiPM ensures that the signal from a single X-ray photon exceeds the noise level of the read-out electronics by a large factor (which is hard to achieve using conventional photodiodes) and allows for a simple pulse processing chain consisting only of current-to-voltage conversion and pulse height discrimination. Since the detector is based on transport of light rather than electric charge and scintillators with high ρ and Z exist, it may provide a solution for the aforementioned issues encountered with semiconductor detectors.

In this contribution, we experimentally investigate the count rate performance of two fast SiPM-based scintillation detectors irradiated by 120 kVp X-ray beams. We compare the outcomes with data from CdTe- and CZT-based PCDs and extrapolate the results to indicate what could be achieved with even faster scintillation detectors. We also study the energy response of the detectors.

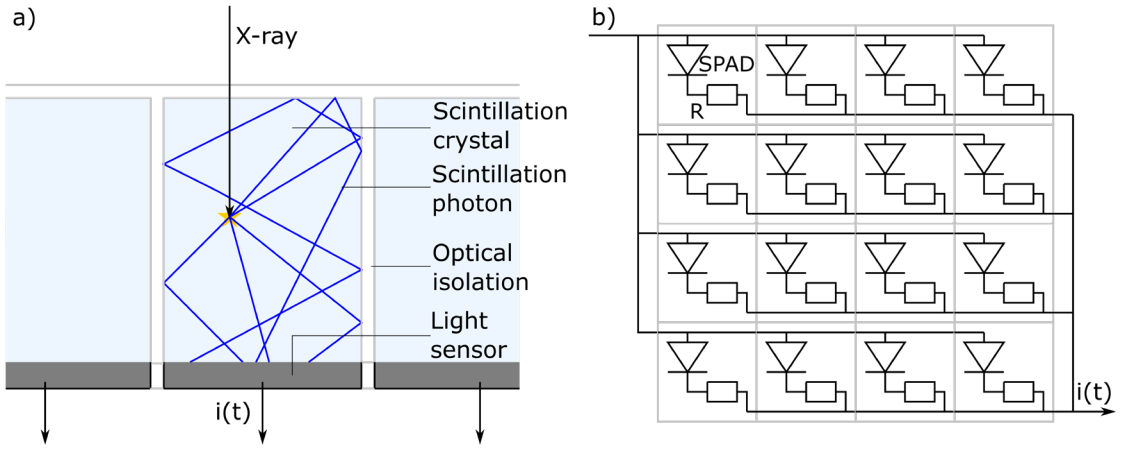

Figure 1. a) Schematic side view of a scintillation detector. Each pixel consists of a scintillation crystal, in which an absorbed X-ray photon is converted into a pulse of optical scintillation photons that typically contains tens of photons per keV of deposited energy. The crystal is one-to-one coupled to a light sensor, which converts the scintillation light pulse into a current pulse $i(t)$. The isotropically emitted scintillation photons are guided towards the light sensor by a reflective optical isolation around the pixel, which also prevents light sharing among multiple pixels (cf. charge sharing in semiconductor detectors). b) Schematic top view of a silicon photomultiplier (SiPM), the light sensor we use in this work. An SiPM is a two-dimensional array of single photon avalanche diodes (SPADs) connected in parallel. Here, only a 4×4 array is shown, but SiPMs have 10^2-10^4 SPADs per mm^2 in practice. When a SPAD detects an optical photon, an avalanche multiplication starts, which is quenched by the resistor R.[8]

2. MATERIALS AND METHODS

We selected two scintillators for this study: $Lu_{1.8}Y_{0.2}SiO_5$:Ce (LYSO, ρ=7.1 g cm^{-3}, Z_{Lu}=71, Shanghai Project Crystal) and $YAlO_3$:Ce (YAP, ρ=5.4 g cm^{-3}, Z_Y=39, Crytur). The former is widely employed in clinical positron emission tomography (PET) detectors, but the latter is a little faster, i.e., τ_d=33 ns versus τ_d=29 ns, as measured by us using the set-up described by Ter Weele et al.[9] We covered a 0.9×0.9 mm^2 pixel of both materials in reflective polytetrafluoroethylene (PTFE, Teflon) powder after having coupled the crystals to 1.0×1.0 mm^2 prototype SiPMs (Broadcom Inc) that have a value of τ_r between 7 ns and 10 ns. The thickness of the LYSO pixel was 1.5 mm (equivalent to 3.0 mm CdTe in terms of X-ray detection efficiency in the diagnostic energy range), whereas the YAP pixel had a thickness of 4.5 mm (equivalent to 1.5 mm CdTe). The current pulses from the detector were converted into voltage pulses without affecting the pulse shape by a trans-impedance amplifier (gain=10) before being digitized by a TeledyneLeCroy HDO9404 oscilloscope (sampling rate=1 GS/s, bandwidth=200 MHz), such that further pulse processing could be done offline.

We calibrated (mean) pulse height as a function of energy for both detectors using five photon emissions (from three radioactive sources): 14 keV (Co-57), 32 keV (Ba-133), 60 keV (Am-241), 81 keV (Ba-133) and 122 keV (Co-57).

X-ray tube experiments were done using an Yxlon Y.TU 320-D03 tube having a tungsten target and an anode angle of 20°. We set the tube voltage to 120 kVp and used a total filtration of 3.0 mm Be and 7.5 mm Al. This yields an incident spectrum ranging from 20 keV to 120 keV. We performed a tube current sweep starting at 0.5 mA and ending at 20 mA, while the detector was at a fixed source-detector distance, and recorded ten pulse trains of 100 ms for each value of the tube current. Figure 2b shows an example of a small part of such a pulse train.

We determined the number of counts in each measurement for two different low-energy counting thresholds, i.e., a 15 keV and a 30 keV threshold, because these usually limit the count rate performance of PCDs. We also determined the number of counts for two different counting algorithms. The first one is paralyzable-like (p-like) counting, i.e., every positive threshold crossing is registered as a count and the maximum voltage before the next negative threshold crossing is a measure of the energy. The second one is nonparalyzable-like (np-like) counting. Here, we evaluate at a fixed time τ_{np} after a count has been registered if the pulse train is still above threshold or not. If yes, then a second count is registered and so on. If not, the next count is registered when the next positive threshold crossing occurs. The maximum signal within the time window τ_{np} is a measure of the energy. To prevent double counting of pulses, τ_{np} should exceed the time-over-threshold of the highest-energy pulses. We therefore used the pulses generated by the full absorption of 122 keV photons from Co-57 to determine the appropriate values of τ_{np} for both detectors and both thresholds (see figure 2c).

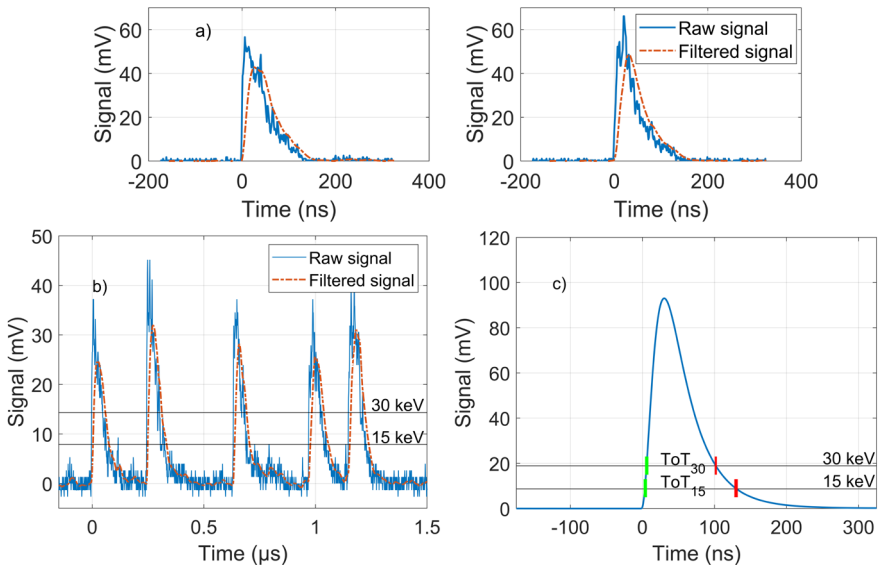

Figure 2. a) Two examples of raw pulses from the LYSO detector in response to a 60 keV photon being fully absorbed in the scintillator and their second order low-pass filtered counterparts. b) An example of a raw and a filtered pulse train from the YAP detector. The 15 keV and 30 keV thresholds are also shown. c) The mean shape of the filtered pulses from the LYSO detector in response to the full absorption of 122 keV photons. Start (green) and end (red) points of the time-over-threshold at 15 keV and 30 keV used to determine the appropriate values of τ_{np} are also visualized.

However, only a few optical photons are detected per keV of deposited energy, so the raw voltage pulses are not perfect convolutions of $A_1\exp(-t_1/\tau_d)$ and $A_2\exp(-t_2/\tau_r)$, but rather show random fluctuations. In order to prevent double counting of single pulses and a degradation of the energy measurement accuracy due to these fluctuations when applying above-mentioned counting algorithms, all recorded signals were smoothened by a second order low-pass filter with a cut-off frequency of 25 MHz before being analyzed. Examples of raw and filtered signals are shown in figure 2a and figure 2b.

3. RESULTS AND DISCUSSION

We derived pulse height spectra from the measurement data obtained by exposing the detectors to the three radioactive sources. An example of such a pulse height spectrum, in this case of Am-241 measured using the YAP detector, is shown in figure 3a. The peak around 2-3 mV originates from SiPM dark counts, which are caused by thermally created e-h pairs that triggered an avalanche multiplication process. The peak next to it is due to characteristic X-rays from the source with energies ranging from 11 keV till 22 keV. Hence, it is possible to distinguish between noise and approximately 10 keV X-ray photons with this type of detector. The third peak in the spectrum corresponds to the 60 keV gamma line of Am-241. It is somewhat asymmetric due to the overlapping K-escape peak at 45 keV.

Figure 3b and figure 3c show the (mean) pulse heights, as determined from Gaussian fits to the pulse height spectra of the Am-241, Ba-133 and Co-57 sources, as a function of energy for both detectors, as well as the non-proportionality relative to 122 keV, i.e., $(V_xE_{122}) / (V_{122}E_x)$, with V the measured pulse height, E the photon energy, and the subscripts indicating the energy-of-interest in keV. The YAP detector has a more proportional response than the LYSO detector. This is an intrinsic property of the scintillator and helps to achieve good energy resolution. Indeed, despite a stronger signal (see figure 3b and figure 3c), i.e., more optical scintillation photons detected, the LYSO detector has a FWHM pulse height resolution of 34% at 60 keV, while the YAP detector achieves 33%, based on a double Gaussian fit that takes into account the K-escape peak at 45 keV (see figure 3a). The distance between the means of the two Gaussians was forced to be equivalent to the 15 keV energy difference between the K-escape peak and the photopeak.

Linear interpolation of the data in figure 3b and figure 3c implies that the 15 keV and 30 keV thresholds of the LYSO detector are at 8.7 mV and 18.9 mV, respectively. For the YAP detector, these thresholds are at 7.9 mV and 14.3 mV.

Based on the mean shape of the pulses due to the full absorption of photons with an energy of 122 keV from the Co-57 source (see figure 2c), the time-over-the x keV threshold (ToT_x) was found to have the following values: $ToT_{15,LYSO}$=128 ns, $ToT_{30,LYSO}$ = 97 ns, $ToT_{15,YAP}$=99 ns, and $ToT_{30,YAP}$=77 ns. Therefore, we used the following values of τ_{np}: $\tau_{np,15,LYSO}$=130 ns, $\tau_{np,30,LYSO}$ = 100 ns, $\tau_{np,15,YAP}$=100 ns, and $\tau_{np,30,YAP}$=80 ns.

The observed count rate (OCR) as a function of tube current I_{tube} is shown in figure 4. We estimated an incident count rate (ICR) for each value of I_{tube} based on the fact that ICR is proportional to I_{tube} and by assuming that ICR for I_{tube}=0.5 mA is equal to OCR as determined by nonparalyzable-like counting with a 15 keV threshold for I_{tube}=0.5 mA. We made sure the pile-up level for I_{tube}=0.5 mA was very low, such that this assumption is reasonable. The top horizontal axes in figure 4 display these estimates. They show that we characterized our detectors up to ICRs of 27-30 Mcps/pixel.

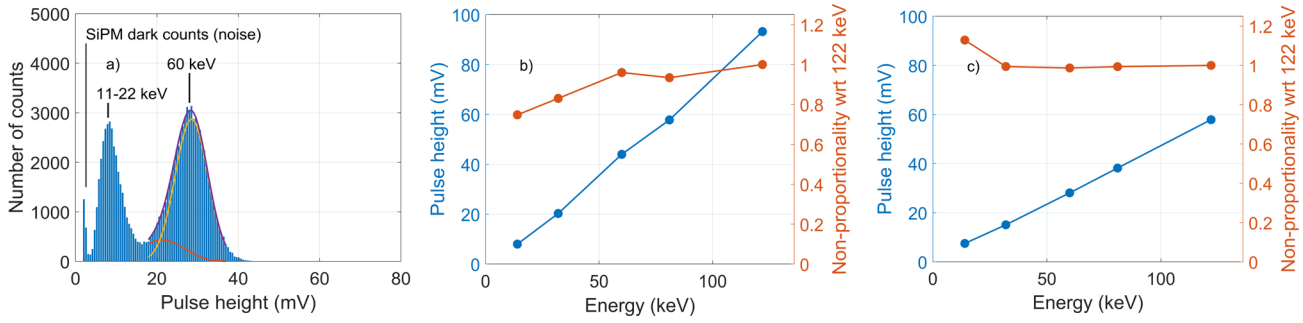

Figure 3. a) A pulse height spectrum of Am-241 measured using the YAP detector, including the double Gaussian fit that takes into account the K-escape peak at 45 keV. We used this fit to determine the mean pulse height and the FWHM pulse height resolution at 60 keV. b) Overview of the (mean) pulse height calibration and the non-proportionality for the LYSO detector. c) The same overview for the YAP detector.

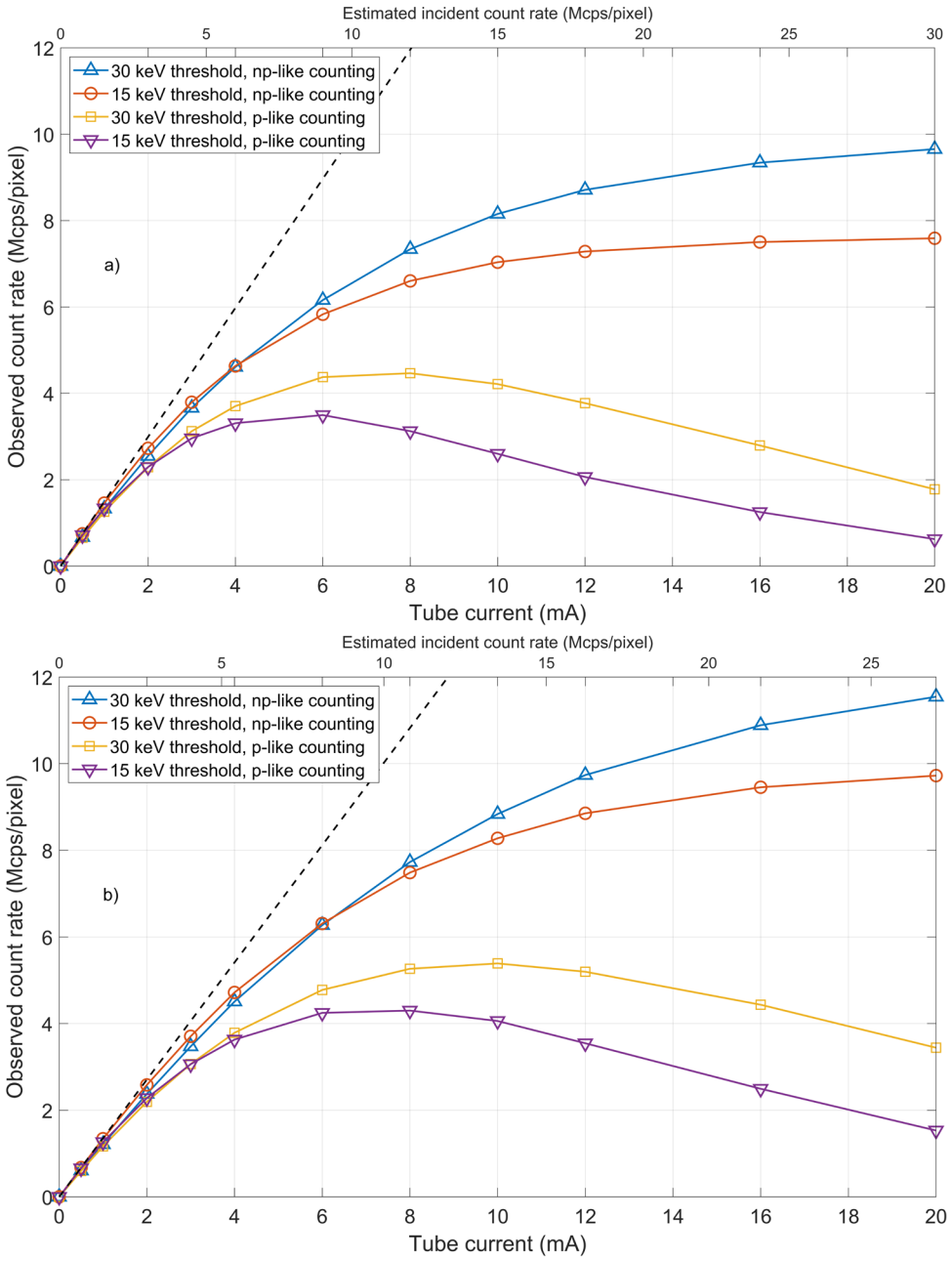

Figure 4. Observed count rate as a function of tube current, counting algorithm, and low-energy threshold for a) the LYSO detector, and b) the YAP detector. The top horizontal axes display our estimates of the incident count rate corresponding to each value of the tube current. The dashed lines represent ideal counting behavior, i.e., observed rate equal to incident rate.

As expected, the curves for p-like counting feature a maximum OCR, which lies between 3.5 Mcps/pixel and 4.5 Mcps/pixel for the LYSO detector, and between 4.5 and 5.5 Mcps/pixel for the YAP detector, depending on the value of the low-energy threshold. The difference between the detectors may not only be explained by a different value of τ_d, but also by the more non-proportional response of LYSO (see figure 3b and figure 3c), such that a pulse generated by a photon of a given energy is longer above a certain threshold in the LYSO detector than in the YAP detector.

Also in accordance with expectations, the curves for np-like counting approach the asymptotes defined by OCR=$1/\tau_{np}$ for high values of I_{tube}, i.e., they approach OCRs of 8-10 Mcps/pixel for the LYSO detector and OCRs of 10-12.5 Mcps/pixel for the YAP detector, again depending on the value of the low-energy threshold.

Although these rate capabilities, combined - if needed - with a reduction of the pixel size to increase the count rate capability per mm^2, may be sufficient for some X-ray imaging applications, CdTe and CZT detectors highly optimized for photon-counting CT aim for a maximum OCR of 10-15 Mcps/pixel in case of p-like counting (e.g., the CZT detector in the prototype scanner of Philips[5]) or an OCR approaching 25-30 Mcps/pixel in case of np-like counting (e.g., the CdTe detector in the prototype scanner of Siemens[4]). The factor limiting the count rate capability of the SiPM-based scintillation detectors investigated here is τ_d. Scintillators with shorter τ_d often have low light yield (the number of scintillation photons generated per keV of deposited X-ray energy), which deteriorates their energy-resolving power. A notable exception is the commercially available scintillator $LaBr_3$:Ce (ρ=5.1 g cm^{-3}, Z_{La}=57, Z_{Br}=35), which combines excellent light yield and energy resolution with a value of τ_d of only 16 ns. Since the higher light yield of $LaBr_3$ can reduce the fluctuations on the pulses that can be seen in figure 2a, such that a filter with a higher cut-off frequency may be used, and the decay time constant of $LaBr_3$ is about two times smaller than that of LYSO and YAP, we expect twice as fast pulses from an $LaBr_3$ detector. We therefore predict a maximum OCR of 9-11 Mcps/pixel for a p-like $LaBr_3$ detector and an OCR approaching 20-25 Mcps/pixel for an np-like one, in case the lowest-energy threshold is set to 30 keV. Such OCRs are close to those of the above-mentioned CdTe- and CZT-based photon-counting CT detectors.

If the pixel size of a scintillation detector is reduced to 0.5×0.5 mm^2 or smaller to achieve higher rate capability per mm^2, the reflective isolation between pixels (see figure 1a) may start to form a relatively large dead area, which limits the achievable OCR and dose efficiency. Space-efficient means of optical isolation are thus required. This has been achieved in the energy-integrating detector of Canon's Aquilion Precision CT scanner. Compared to the company's standard CT detector, the pixel dimensions have been reduced by a factor two, so the number of pixels per mm^2 has been increased by a factor four. The thickness of the reflective septa has been reduced accordingly, such that the dose efficiency of this detector (with 0.25×0.25 mm^2 pixels at the isocenter) is hardly affected. Even dead area-free options exist, such as a columnar microstructure of the scintillator[10] (cf. the CsI scintillator in flat panel detectors), which may be applied to further reduce the pixel size, although at the cost of some light sharing among multiple pixels.

Lastly, figure 5 shows examples of spectra measured using the LYSO and YAP detectors, for I_{tube}=0.5 mA (i.e., for low incident rates), a 15 keV threshold, and p-like counting. From left to right we observe the typical features of an X-ray tube spectrum: A rising edge at low energies, although with relatively many counts, which is probably due to K-escape events, followed by an intense peak caused by the K X-rays of the tungsten target of the X-ray tube, and then a gradually decreasing spectral intensity towards the maximum energy of 120 keV, with some overflow to higher energies because of the finite energy resolution of the detectors and perhaps some pulse pile-up.

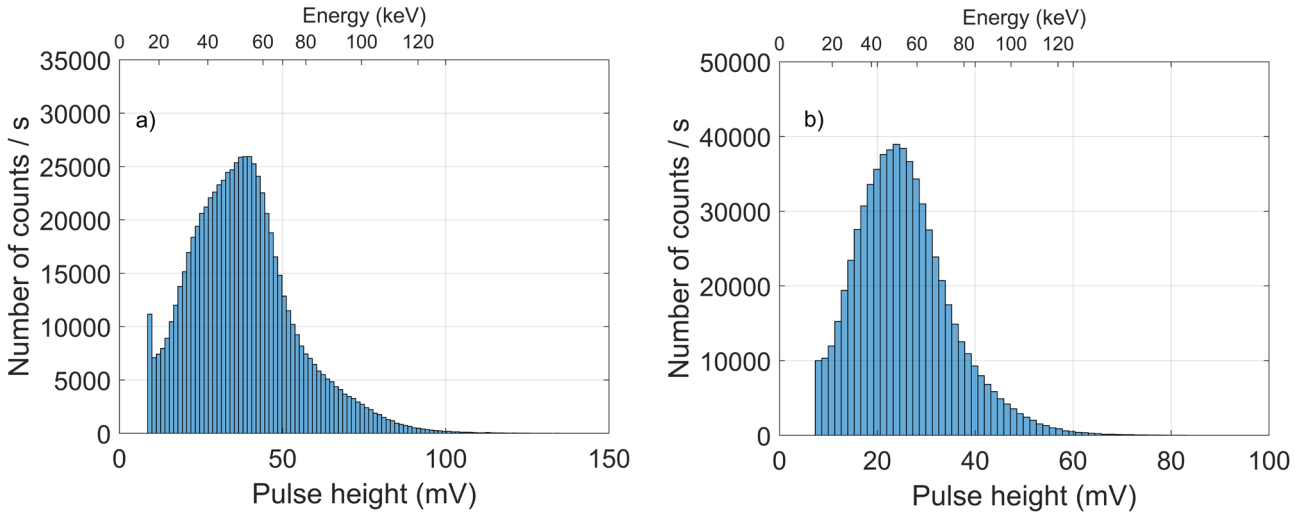

Figure 5. X-ray tube spectra (120 kVp, tungsten anode, anode angle of 20°, 3.0 mm Be and 7.5 mm Al filtration) measured using a) the LYSO and b) the YAP detector, for p-like counting with a 15 keV threshold at a tube current of 0.5 mA, i.e. under low fluence rate conditions. The energy-axes are based on the calibrations shown in figure 3b and figure 3c.

4. CONCLUSIONS

We introduced fast SiPM-based scintillation detectors as potential alternatives to direct-conversion detectors for (medical) X-ray photon-counting applications. Using an X-ray tube operating at 120 kVp, we experimentally studied the energy response and the count rate capability of two 1×1 mm^2 single-pixel detectors based on the fast and commercially available scintillators LYSO and YAP and an ultrafast SiPM prototype. The measured spectra at low fluence rate showed signs of the typical features of an X-ray tube spectrum. For paralyzable-like counting and a 30 keV threshold, we found maximum observed count rates (OCRs) of 4.5 Mcps/pixel (LYSO) and 5.5 Mcps/pixel (YAP), whereas the OCRs approached 10 Mcps/pixel (LYSO) and 12.5 Mcps/pixel (YAP) for nonparalyzable-like counting and a 30 keV threshold. Although this performance may be sufficient for some X-ray photon-counting applications, CdTe- and CZT-based direct-conversion detectors highly optimized for photon-counting CT achieve at least twice as high OCRs. However, extrapolating the present results, we expect that the performance of a detector based on the twice as fast and commercially available $LaBr_3$ scintillator and the same ultrafast SiPM prototype can come close to that of the aforementioned CdTe and CZT detectors. We furthermore pointed towards two possible solutions for dose-efficient pixel size miniaturization, namely very thin reflectors and scintillators grown with a columnar microstructure, which allow to further increase the count rate capability per mm^2 if required so by the application.

REFERENCES

[1] Hsieh, S.S. et al., "Photon Counting CT: Clinical Applications and Future Developments", IEEE Transactions on Radiation and Plasma Medical Sciences 5(4), 441-452 (2020). doi: 10.1109/TRPMS.2020.3020212

[2] Flohr, T. et al., "Photon-Counting CT Review", Physica Medica 79, 126-136 (2020). doi: 10.1016/j.ejmp.2020.10.030

[3] Persson, M. et al., "Upper Limits of the Photon Fluence Rate on CT Detectors: Case Study on a Commercial Scanner", Medical Physics 43(7), 4398-4411 (2016). doi: 10.1118/1.4954008

[4] Kappler, S. et al., "Photon Counting CT at Elevated X-ray Tube Currents: Contrast Stability, Image Noise, and Multi-Energy Performance", Proceedings of SPIE 90331C (2014). doi: 10.1117/12.2043511

[5] Steadman, R. et al., "ChromAIX2: a Large Area, High Count-Rate Energy-Resolving Photon Counting ASIC for a Spectral CT Prototype", Nuclear Instruments and Methods in Physics Research Section A 862, 18-24 (2017). doi: 10.1016/j.nima.2017.05.010

[6] Da Silva, J. et al., "Resolution Characterization of a Silicon-Based, Photon-Counting Computed Tomography Prototype Capable of Patient Scanning", Journal of Medical Imaging 6(4), 043502 (2019), doi: 10.1117/1.JMI.6.4.043502

[7] Roy, U.N. et al., "Role of Selenium Addition to the CdZnTe Matrix for Room-Temperature Radiation Detector Applications", Scientific Reports 9, 1620 (2019). doi: 10.1038/s41598-018-38188-w

[8] Van der Sar, S.J. et al., "Silicon Photomultiplier-Based Scintillation Detectors for Photon-Counting CT: a Feasibility Study", Medical Physics 48(10), 6324-6338 (2021), doi: 10.1002/mp.14886

[9] Ter Weele, D.N. et al., "Intrinsic Scintillation Pulse Shape Measurements by Means of Picosecond X-ray Excitation for Fast Timing Applications", Nuclear Instruments and Methods in Physics Research Section A 767, 206-211 (2014). doi: 10.1016/j.nima.2014.08.019

[10] Bhandari, H.B. et al., "Large-Area Crystalline Microcolumnar $LaBr_3$:Ce for High-Resolution Gamma-Ray Imaging", IEEE Transactions on Nuclear Science 60(1), 3-8 (2013). doi: 10.1109/TNS.2012.2213612